Measurements in Turbulent Swirling Flow Through an Abrupt Axisymmetric Expansion

P. A. Dellenback,* D. E. Metzger,† and G. P. Neitzel‡
Arizona State University, Tempe, Arizona

Experimental data are presented for both axial and tangential velocity components in turbulent swirling flow downstream of an abrupt 1:2 expansion. Measurements of mean and rms velocities were performed in a water flow with a laser Doppler anemometer. In the upstream tube, the Reynolds number was varied from 30,000 to 100,000 and the swirl number from zero to 1.2. For low swirl levels, as the core flow passed through the expansion, it departed the axis of symmetry and precessed about that axis at frequencies on the order of 1 Hz. As swirl was increased to moderate levels, the flow became axisymmetric with on-axis recirculation marking the onset of vortex breakdown. At the highest swirl levels, flow on the tube centerline was in the same direction as the mean flow, with reverse flow occurring just off-axis. Turbulence intensities at the highest swirl levels were found to reach 60%. As the swirl was increased from zero to its maximum value, the flow reattachment point moved upstream from 9 to 2 step heights.

Nomenclature

D,D_2 = diameters of upstream and downstream tubes, respectively
f = precession frequency of PVC
h = step height, $(D_2 - D)/2$
k = tubulence kinetic energy
l = turbulence length scale
PVC = precessing vortex core
Q = volumetric flow rate
r = radial coordinate
R,R_2 = radius of upstream and downstream tubes, respectively
Re = Reynolds number in upstream tube, $\bar{U}D/\nu$
S = swirl number in upstream tube, see Eq. (1)
TI = rms velocity normalized with U_1 (*100)
U = local mean axial velocity
$\bar{U}$ = axial velocity averaged over cross section
U_1 = maximum axial velocity in upstream tube
V = local mean tangential velocity
u',v' = axial and tangential rms velocities, respectively
X = axial distance from expansion face
x_r = reattachment length
y = thickness of viscous sublayer
β = ratio of D/D_2
ν = molecular viscosity of fluid

Introduction

TURBULENT swirling flow through an abrupt axisymmetric expansion is a complex flow possessing several distinctly different flow regimes, either one or two recirculation regions, extremely high levels of turbulence, and periodic asymmetrics under some conditions. An accompanying elevation of heat-transfer rates is a principal motivation for the addition of swirl to flows in dump combustors of gas turbine engines and in solid-fuel ramjet combustors. The objective of the present investigation was to examine experimentally these flowfields in some detail.

The sudden-expansion geometry produces mixing rates downstream of the expansion that are substantially higher than those that would be obtained at the same Reynolds number in the entrance region of a pipe. This enhancement in mixing occurs in spite of a recirculation region extending about nine step heights downstream from the expansion. In this recirculation region, mean velocities are typically only 10% as high as those found in the core flow. The elevated mixing rates are due to very high levels of turbulence kinetic energy generated by shearing as the core flow issues into the larger pipe. Near the tube wall, where length scales are small, dissipation dominates because the dissipation is inversely proportional to the length scale. But, in the high-shear regions away from the wall, length scales are large and dissipation rates consequently low. Thus, turbulence kinetic energy generated in the shear layer dissipates relatively slowly, and its levels are much higher than would be found in ordinary pipe flow, where no such internal shear layer exists. High turbulence kinetic energy levels also cause the thickness of the (molecular) viscosity-dominated sublayer to be reduced. Specifically, for flows where the principal energy generation is not at the wall, but rather removed from it as in the sudden-expansion flowfield, Spalding[1] suggested that the viscous sublayer thickness (y) changes with the turbulence kinetic energy (k), so that the sublayer Reynolds number ($yk^{1/2}/\nu$) is a universal constant. Hence, the sublayer will become thinner with increasing levels of turbulence kinetic energy.

There has been speculation[2] that a small, counter-rotating corner eddy lies very close to the face of the expansion. Mean velocities in the corner eddy are of the order 0.01 U_1 according to Ref. 2, but there are apparently no velocity measurements or flow visualization results in the literature that either confirm this value or support the existence of this feature in the axisymmetric-expansion flowfield. However, in a series of heat-transfer measurements, Baughn et al.[3] speculated that small and consistent minima in Nusselt numbers near the face of the expansion were possible evidence for the presence of a corner eddy. The hypothesized corner eddy is likely to continue to defy direct velocity measurement since the available instrumentation consists of comparatively large probes or probe volumes for detection of such a small feature in this restrictive geometry.

Adding swirl to the sudden-expansion flowfield causes an increase in the width, growth rate, entrainment, and decay of the core flow emanating from the upstream tube. It is also

Received March 2, 1987; revision received Nov. 25, 1987.

*Research Associate; currently, Assistant Professor, Southern Methodist University, Dallas, TX.
†Professor.
‡Associate Professor.

found that on-axis recirculation (known as vortex breakdown[4]) may occur for sufficiently high swirl strengths. This recirculation is driven by an adverse pressure gradient on the tube centerline that results from the viscous dissipation of the tangential velocity component as the flow proceeds downstream. As swirl strength is increased from zero, the vortex breakdown may first be seen as an on-axis ellipsoid of recirculating fluid. As the degree of swirl is further increased, the ellipsoid may stretch in the downstream direction and form a tube of recirculating fluid, at least in the sudden-expansion geometry.

A further complex and little-understood phenomenon that frequently occurs in swirling flows is the existence of an unsteady (although usually periodic) asymmetry in the flowfield. These asymmetries are usually associated with the vortex breakdown phenomenon and on-axis recirculation.[4] Consequently, they are usually observed at moderate-to-large swirl strengths. However, the present investigation documents an asymmetry like that observed by Hallett and Gunther,[5] which occurs at low swirl strengths in the absence of on-axis recirculation. This latter flow asymmetry is characterized by the vortex emanating from the upstream tube departing the axis of symmetry and then precessing about that axis. This feature will be referred to here as the precessing vortex core (PVC) after Gupta et al.[6]

Analytical prediction of the present flowfield is sufficiently complex that it is manageable only if the flow is assumed to be steady and axisymmetric. With these simplifications, there is no potential for predicting the unsteady three-dimensional asymmetry that occurs. Furthermore, Sultanian and co-workers[7] in their recent computations of this flow had difficulty in accurately predicting the extent of the on-axis recirculation zone and turbulence intensities downstream of the expansion. Sultanian also found his model to be quite sensitive to the inlet conditions, especially turbulence intensity. With this in mind, we present measurements upstream of the sudden expansion to facilitate subsequent modeling efforts.

At this point, it is convenient to define several scales and independent variables that will be used in the following discussion. There are two length scales required in the axisymmetric sudden-expansion problem. The first is the step height (h), which experience has shown to be reasonably well suited to correlation of reattachment lengths. A second necessary length scale is either the upstream or downstream tube diameter. Here, the upstream tube diameter (D) is employed. The Reynolds number is based on the diameter of the upstream tube and the average velocity in the upstream tube. Swirling flows are commonly characterized by the following definition for a device-independent swirl number:

$$S = \frac{1}{R}\frac{\int_0^R r^2 UV\,\mathrm{d}r}{\int_0^R rU^2\,\mathrm{d}r} = \frac{\int_0^1 (r/R)^2 UV\,\mathrm{d}(r/R)}{\int_0^1 (r/R)U^2\,\mathrm{d}(r/R)} \tag{1}$$

The swirl number may be physically interpreted as the ratio of axial fluxes of swirl and linear momentum divided by a characteristic radius.

Previous Investigations

Sudden Expansion Flow Without Swirl

Axial flow through a sudden axisymmetric expansion is a fairly well studied problem[8–13] that represents the limiting case of zero swirl against which current results can be compared. The widely referenced set of data by Chaturvedi[8] includes mean velocities and turbulence quantities measured with a hot-wire anemometer. However, a check of Chaturvedi's mass balances yields profile-to-profile variations as high as 30%. Chaturvedi attempted to smooth the data, but the arbitrary nature of this correction reduces one's confidence in it. Freeman[9] used a laser Doppler anemometer (LDA) to measure axial mean velocity and turbulence intensity, while Moon and Rudinger[10] report only an axial mean velocity from their LDA measurements. Yang and Yu[11] report turbulence quantities and mean velocities, also obtained with an LDA, but the validity of their data has been called into question recently[14] because of significant mass balance discrepancies that are actually higher than those quoted in the paper. Among the various studies, the measurements of Gould et al.[12] and Stevenson et al.[13] appear to be the most complete and the most closely related to the present work.

The present state-of-the-art of computational flow modeling is such that the sudden-expansion problem (purely axial flow) is now fairly well handled by various schemes. The reader is referred to Gosman et al.[15] and Stevenson et al.[13] for discussions of k-ε modeling and to Minh and Chassaing[16] and Sultanian et al.[7] for application of Reynolds stress modeling to this problem.

Axisymmetric Expansion with Swirl

There have been several recent investigations reporting measurements in swirled flows through sudden expansions,[17-20] but all have used intrusive probes, even though it is known that such probes can significantly alter flowfields with recirculation. In fact, these studies are concerned primarily with the development of measurement techniques using five-hole pitot tubes and hot-wire anemometry for application in multidimensional complex flows. Consequently, these four papers might be considered work in progress on the development of measurement techniques rather than a collection of results available for comparison purposes.

Vortex Breakdown and the PVC

There have been a number of analytical investigations of vortex breakdown (see reviews by Hall[21] and Leibovich[22]), but the asymmetries in swirled flows are so complex and irregular that these analytical treatments have been mostly unsuccessful. Thus, the primary body of information about unsteady asymmetries in swirling flows has been gathered in experimental studies.[4, 23–26]. The flow geometries in these experiments are all axisymmetric, but a wide variety of configurations are represented. These include straight tubes,[23] diffusers,[4, 25, 26] sudden contractions,[23] and unconfined swirling jets.[24] Although the geometries are diverse, the nature of the asymmetrical flows observed in the various experiments is remarkably similar. The single feature common to all of these flows is a precession of the flow about the tube axis in conjunction with vortex breakdown.

All of the prior vortex breakdown experiments were essentially flow visualization studies. In those cases where hot-wire and laser Doppler anemometry were employed,[4, 23, 24] these techniques were used to look for a sinusoidal variation in mean velocity as the asymmetry swept past the point of measurement. Cassidy and Falvey[23] noted that the precession frequency was independent of Reynolds number for $Re \geq 10^5$. In very careful flow visualization studies, Faler and Leibovich[4] identified six distinct disturbance modes whose flow regimes could be characterized by Reynolds and swirl numbers. The experiments of Faler and Leibovich led them to conclude that there are no truly axisymmetric disturbance patterns in these flows.

There is an important distinction between the papers mentioned in the preceding paragraphs and the work of Hallett and Gunther.[5] In the previously mentioned studies, the flow asymmetries occur only in conjunction with vortex breakdown, but Hallett and Gunther's PVC in a sudden expansion occurs only for swirl strengths below those associated with vortex breakdown. In fact, with increasing swirl, the periodicity of the PVC became weaker and less distinct until, just before onset of vortex breakdown, it disappeared altogether. Also, they noted that precession was strongest and most regular at low swirl whereas,

at higher swirl, the motion became increasingly irregular. Hallett and Gunther observed that the amplitude of the PVC dissipated with increasing downstream distance as the PVC became more coincident with the tube axis. Finally, they report no evidence of flow asymmetry upstream of the expansion in velocity measurements made with a five-hole pitot probe.

Experimental Apparatus

A water flow loop, constructed of stainless steel and shown schematically in Fig. 1, comprised the main element of the test facility. Swirl was generated by supplying a variable portion of the flow through tangential slots as indicated by Fig. 2. Inside diameters of the axial inlet tube, the swirler insert, and the upstream test section were 5.08 cm. The axial inlet tube was 31 diameters long to allow axial flow development, and the sudden expansion was 15 diameters downstream of the swirl generator. Flow rates to the slots and the axial inlet tube could be controlled independently, thus providing the capability to vary swirl strength continuously. Flow rates were measured with turbine-type flowmeters. An in-line filter was used to remove particles nominally larger than 1 μm from the water.

The tube upstream of the expansion was made of Plexiglas, which was bored, honed, and polished to a final inside diameter of 5.078 ± 0.008 cm. To allow LDA measurements close to the expansion, the tube and attached expansion face extended into the downstream tube so that structural flanges and bolts did not interfere with the laser beams. Measurements were thus possible 1 cm downstream of the expansion. The downstream tube was not machined or honed owing to complications associated with its relatively large size. Consequently, it was very slightly oval, with an inside diameter of 9.850 ± 0.020 cm and an outside diameter of 10.767 ± 0.003 cm. Thus the expansion ratio was 1:1.94. The length of the downstream tube was 1.04 m.

LDA Optical System

The laser Doppler anemometer was a conventional single-component system operated in the dual-beam mode. The system included a 15-mW He-Ne laser, a Bragg cell for frequency shifting of one beam, and beam-expansion optics to minimize probe volume size. The optical components produced an ellipsoidal probe volume whose nominal $1/e^2$ extent was 0.91 mm long and 0.09 mm in diameter.

Both transmitting and forward-scatter receiving optics were mounted on a single aluminum channel which, in turn, was rigidly affixed to the table of a three-axis milling machine. To obtain the desired 1-m travel in the axial direction, it was necessary to fasten the milling table to four precision linear bearings, which rode on two parallel steel shifts. A dial indicator was used to monitor the radial position of the probe volume.

Experimental Procedures

Artificial seeding of the flow was not required. The test loop was filled with tap water having a relatively high mineral and particulate content. The water was filtered briefly after each filling of the loop to remove particles nominally larger than 1 μm. Filtering to this size was consistent with the Melling and Whitelaw[27] suggestion that particulates smaller than 10 μm will adequately follow the flow up to frequencies of 500 Hz. For most water flows, the bulk of the energy-containing eddies have frequencies in this range.

Both axial and tangential components of mean velocity and rms turbulence levels were measured on a dense grid of points lying in a horizontal plane through the tube centerline. Included in the grid of measurement stations were two upstream locations at $X/D = -2.0$ and -0.5. Locations for profiles in the downstream tube were chosen to optimize resolution in the near-expansion region, where velocity and turbulence levels change rapidly with X/D. Corrections for optical refraction of the laser beams at the air-Plexiglas and Plexiglas-water interfaces[28] were employed to locate the probe volume at even intervals in the radial direction. For most cases with swirl, profiles were made across the entire tube to check for flow asymmetry, even though asymmetry was found only in the subcritical-swirl flows.

Measurements at radius ratios ± 0.95 were attempted for all profiles. However, measurement close to walls is generally difficult because scattered light from the walls results in poor signal-to-noise ratios. In the present work, spurious wall reflections were largely overcome by collecting scattered light at

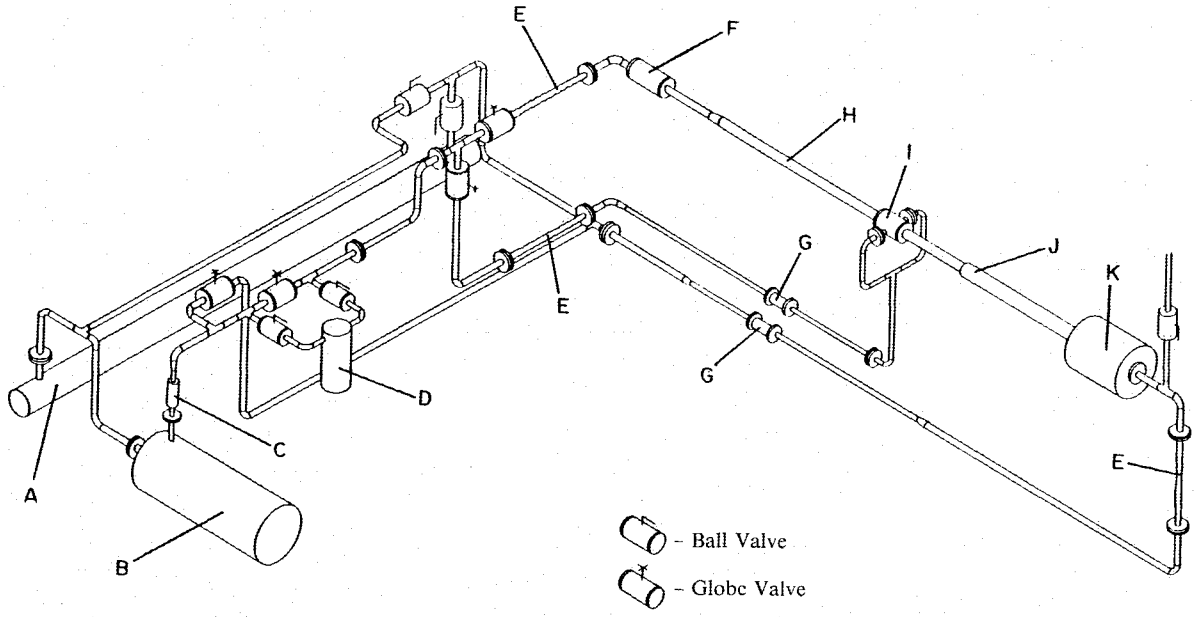

Fig. 1 Schematic of flow loop.

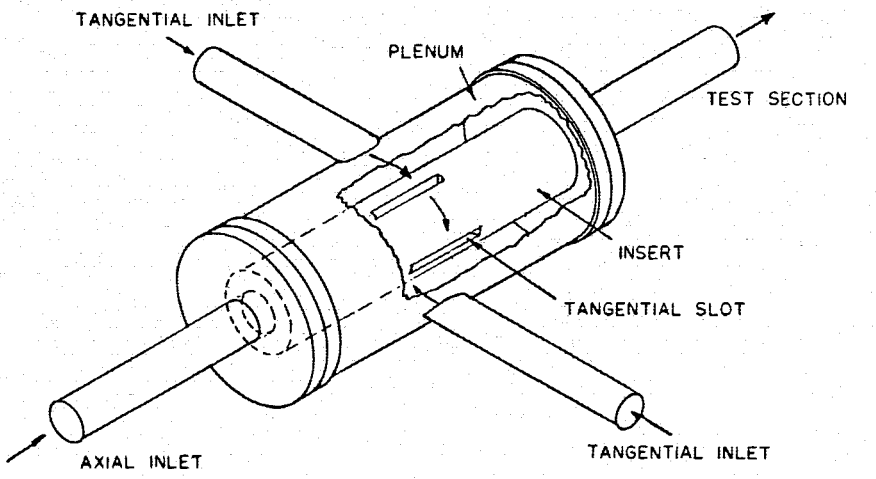

Fig. 2 Detail of swirl generator.

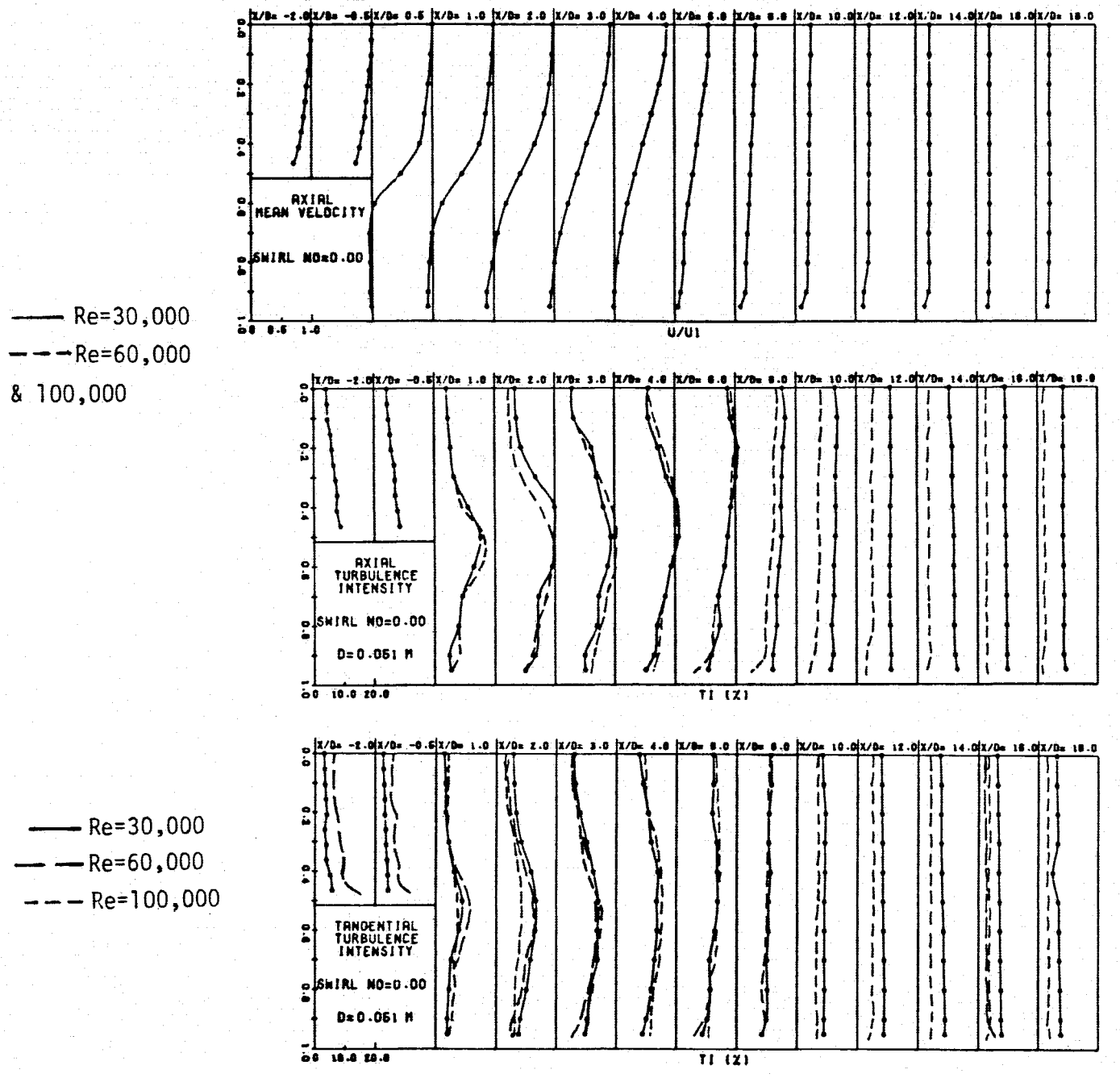

Fig. 3 Velocity field; $S = 0$.

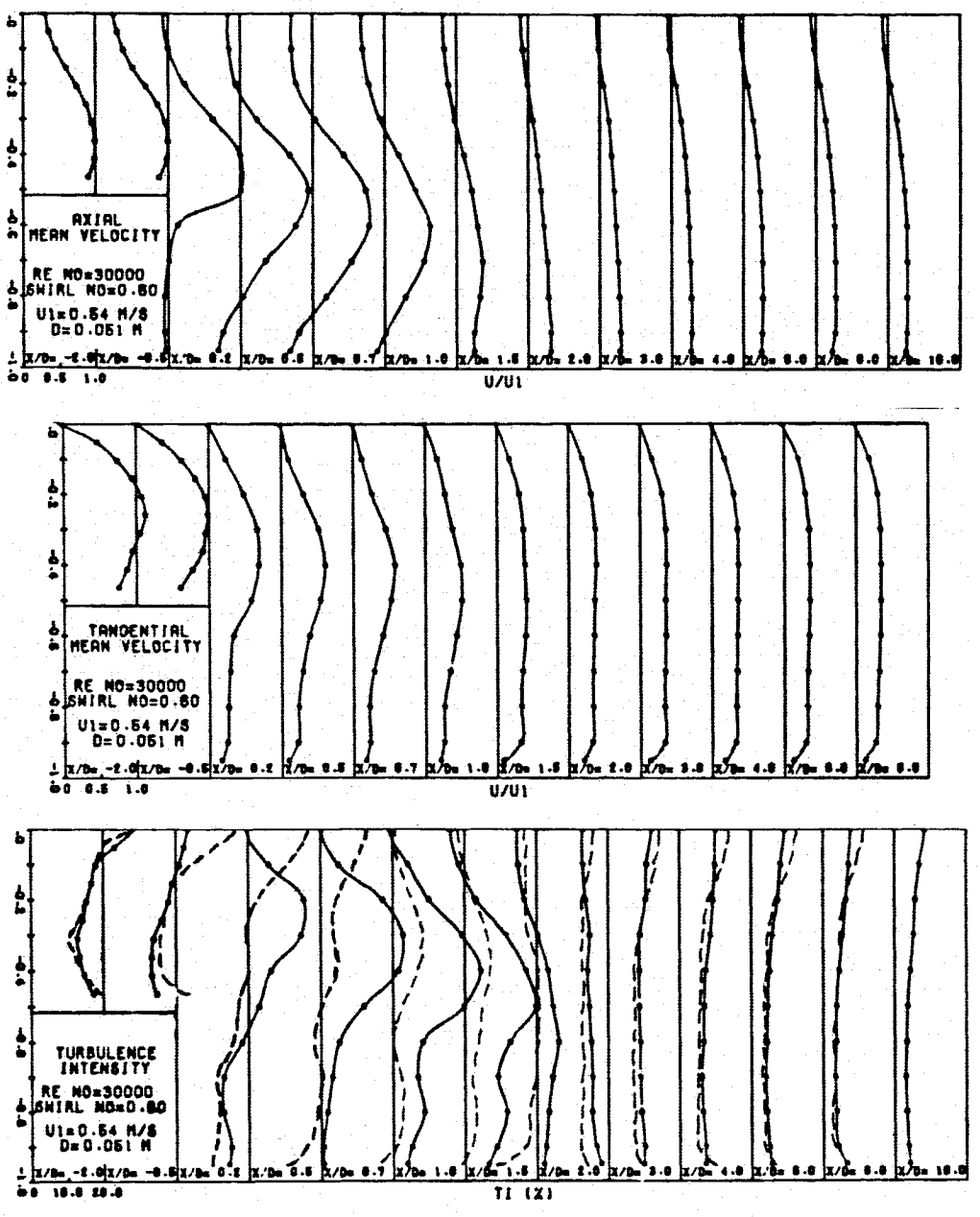

Fig. 4 Velocity field; Re = 30,000, S = 0.60: —— axial TI; ---- tangential TI.

about 5 deg off the forward-scatter axis, thus truncating the probe volume slightly and keeping the light-collection optics out of the horizontal plane, which contains most of the disruptive stray light. Using this technique, results at $r/R_2 = \pm 0.95$ in the downstream tube were consistent and credible. In the upstream tube, because of its smaller size, the same degree of credibility extended only to $r/R = \pm 0.90$.

Velocity biasing was eliminated by random sampling in the present experiments. Durao et al.[29] suggest that, for data collection percentages of less than 40%, the average velocity obtained will be less than 2% higher than the true mean velocity. Stevenson et al.[13] suggest that the velocity bias will be effectively eliminated for collection percentages on the order of 1%. For this work, a computer sampled the output from a counter processing device at a rate of 130 Hz. Data rates often fell to about 4000 Hz at the near-wall grid points of $r/R_2 = \pm 0.95$ but usually ranged from 8000 to 40,000 Hz elsewhere. Hence, the worst-case collection percentages were about 3% near the tube walls. The waiting period also minimizes the potential bias caused by a single particle generating multiple measurements before leaving the probe volume.

Mean and rms velocities were determined from sample sizes of 4000 data points. The statistical error[30] associated with this sample size is $\pm 1\%$ in the mean-velocity measurement for a local turbulence intensity (TI) of 70% and about $\pm 2\%$ in the measurement of TI. A worst-case computation of the spatial velocity biasing due to the finite probe-volume size[31] suggests that the spatially averaged TI is only 0.6% higher than the TI at the probe volume's center.

Investigation of the PVC

The experimental examination of the precessing vortex core and the vortex-breakdown bubble consisted of both flow visualization and selective probing with LDA. Some modest success in visualizing the flow was obtained using air bubbles and high-intensity lighting in two different procedures. The first and more useful method was to introduce approximately 1 liter of air into the 250-liter capacity of the test loop. The air and water were then mixed by operating the loop for a short time. The ensuing air bubbles were so small as to be almost invisible to the eye with ordinary room lighting but, with the use of a

high-intensity photographic light source, a "mist" of bubbles could be seen well enough to reveal qualitative details of the flow. These bubbles were sufficiently small that they showed no discernible tendency either to rise to the top of the tube or to collect on the tube centerline but seemed rather to follow the flow. When the flowfield was visualized in this fashion, it was often difficult to determine what was happening in the tube. In particular, while it was clear that the vortex from the upstream tube was entering the downstream tube asymmetrically and precessing, vigorous activity in the near-wall recirculation zone complicated the examination so that the direction of precession at very low swirl numbers ($S \leq 0.15$) could not be determined. To aid in the resolution of this dilemma, air was injected through a small total-pressure probe on the centerline of the upstream tube. The air-injecting probe was located just downstream of the swirl generator. As the larger bubbles that were produced in this way moved downstream, they were pinned on the tube centerline by centrifugal forces. As they passed through the expansion, they marked the vortex axis and thus revealed the direction of vortex precession.

Precession frequency information was gathered by monitoring the counter-processor's analog output on both a stripchart recorder and a spectrum analyzer to obtain a real-time variation of mean velocity. An rms voltmeter with adjustable time constant was connected between the counter's output and the recorder or analyzer so that the higher frequencies associated with turbulent fluctuations could be filtered out.

The methods of Kline and McClintock[32] were employed to determine that the largest uncertainties were about 2% in Reynolds number, 8% in swirl number, 10% in Strouhal number, and 1% in probe volume positioning. Uncertainties in mean and rms velocities stemming from the many possible biases and broadening errors are estimated to be about $\pm 3\%$ and $\pm 10\%$, respectively.

Results and Discussion

Velocity and TI Distributions

The results for U, u', and v' for unswirled flow at Reynolds numbers of 30,000, 60,000, and 100,000 are shown in Fig. 3. The mean and fluctuating velocities in Fig. 3 have been normalized with the axial centerline velocity occurring in the upstream tube. Mean velocities for the three Reynolds numbers collapse to single curves, but when the regions far downstream ($X/D = 18$) are examined, it can be seen that the turbulent fluctuations have apparently dissipated faster for larger Reynolds numbers (the TI for $Re = 60{,}000$ and $Re = 100{,}000$ were virtually identical). Figure 3 indicates that the axial TI has decreased to a nominal background level of about 2.5% for $Re = 100{,}000$ while it remains near 8% for $Re = 30{,}000$. The difference in TI's is due to higher rates of dissipation at the larger Reynolds numbers. Dissipation usually scales as u'^3/ℓ, or $(u'/U)^3/(\ell/U^3)$ so that, for length scales (ℓ) and turbulence intensities ($u'/U * 100$) of the same order, dissipation increases with increasing U or increasing Reynolds number.

For unswirled flows, we see that a state of near isotropy in u' and v' exists at $X/D = -2.0$, and then again far downstream after the flow has redeveloped. However, throughout much of the intermediate region, the axial TI is approximately 30% greater than the tangential TI. The peak values for both of these quantities are generally coincident and lie in the region bounded by the edge of the shear layer and the tube centerline. For each Reynolds number, these maximum values are on the order of 20–22% for axial TI and about 15% for tangential TI. This maximum value (and the distributions of U and u') compare very favorably with the work of Stevenson et al.,[13] who report a maximum axial TI of 22%.

Swirled-flow data for five supercritical-swirl cases are shown in Figs. 4–8. For these highly swirled flows, the maximum axial velocity in the upstream tube (U_1) occurred near $r/R \approx 0.8$, and it is this value that is used for the normalization of mean and rms velocities. Figures 4–8 demonstrate a large influence of the downstream flow on the $X/D = -0.5$ profiles for all supercritical-swirl cases. The influence is especially strong on the TI's whose magnitudes and distributions are changed dramatically from the $X/D = -2.0$ station. The turbulence intensities continue to be highly nonisotropic in the downstream tube for all the supercritical-swirl flows. These results have important ramifications on the modeling of this flow because they imply that the frequently used k-ε model, with its assumption of isotropy, will be unable to predict accurately the observed features of highly swirled flows.

The highest swirl strength achieved in this set of experiments is shown in Fig. 8, where we see two features not present in the flows with lower swirl numbers. The first is that, as the flow development proceeds downstream from $X/D = 4$, the centerline velocity is positive with recirculation just off-axis. We also find that the on-axis tangential velocity gradient is steepening throughout the downstream tube, consequently producing greater shearing and ever-increasing turbulence intensities. Both of these trends continued through $X/D = 18$. These two features cannot be wholly discerned from the data presented for $Re = 60{,}000$, $S = 1.16$ but, from Fig. 6 and measurements made further downstream (those for $X/D > 10$ not shown

Table 1 Reattachment lengths

Present investigation		
Reynolds no.	Swirl no.	x_r/h
30,000	0.00	9.3
	0.60	2.5
	0.98	1.9
60,000	0.00	9.2
	0.77	2.2
	1.16	1.8
100,000	0.00	9.0
	0.74	2.2
	1.23	1.8

Investigator	Method	Media	β	$Re(UD/\nu)$	x_r/h
Chaturvedi[8]	Hot-wire	Air	0.50	200,000	9.2
Freeman[9]	LDA	Water	0.48	63,000	8.8
Moon & Rudinger[14]	LDA	Air	0.70	280,000	8.8
Gould et al.[12] and Stevenson et al.[13]	LDA	Air	0.50	90,000	8.6
Yang and Yu[11]	LDA	Air	0.37	53,000	9.2

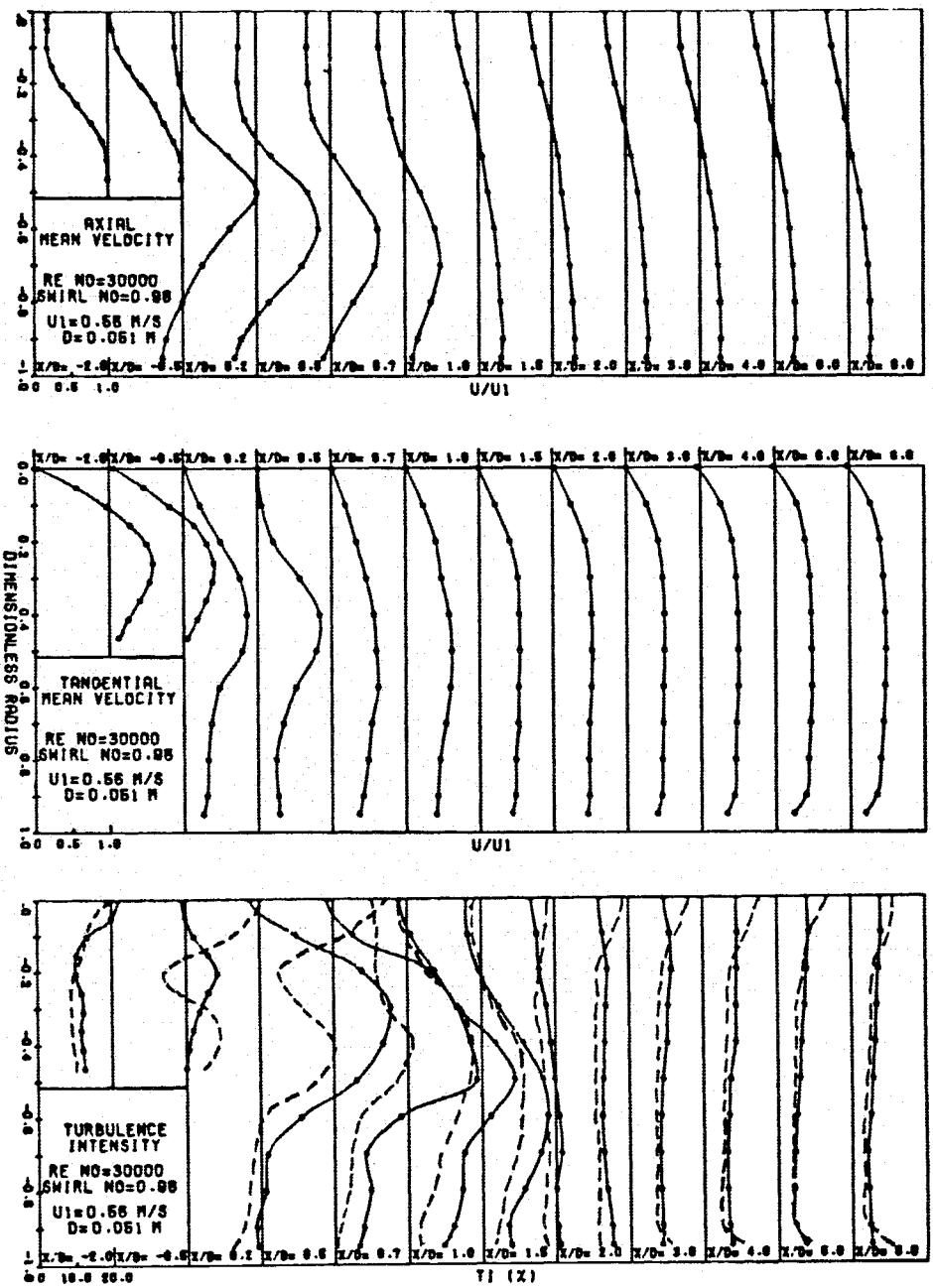

Fig. 5 Velocity field; Re = 30,000, S = 0.98: ——— axial TI; ---- tangential TI.

here), the trends toward positive centerline velocity and continuously increasing TI do seem to be present and hence consistent with the Re = 100,000, S = 1.23 data. That centerline TI's continue to increase to the end of the test section is a limitation of the test section's length. In a longer tube, the decay of swirl would give rise to a maximum in TI at some axial location. However, it is perhaps surprising that this flow condition, with its high diffusion rates and relatively short wall recirculation zone, is still evolving so far downstream at $X/D = 18$.

For the swirled flows in general, the peak value for axial TI always occurs in the shear layer near $r/R_2 = 0.5$, and the maximum value of tangential TI is always found along the tube centerline. For the swirled flows, there is a considerable divergence in the behaviors of axial and tangential turbulence intensities for $X/D = -0.5$ and throughout the downstream tube. It can be seen from Figs. 4–8 that, along the tube centerline, the tangential TI is typically twice the axial TI. At the same time in the shear layer around $r/R_2 = 0.5$, the axial TI is commonly twice the tangential TI. The largest axial TI's are on the order of 45% for moderate swirl ($0.60 < S < 0.77$) and 58–65% for high swirl ($0.98 < S < 1.23$). In each case, the corresponding maximum tangential TI is always several percent less than the axial value. For the swirled flows, these maximum values were found near $X/D = 0.5$ whereas, for the unswirled flows, they were found between $3 < X/D < 6$.

A composite of axial centerline velocities is shown in Fig. 9. For the unswirled flows, the flat portion of the curve for $X/D > 12$ indicates that the velocity profile has redeveloped. From an area-ratio argument, one would anticipate that, for the present expansion ratio of 0.51, the normalized centerline velocity would achieve a downstream value of $(0.51)^2$ or 0.265. The actual value reached was a consistent 0.24, which suggests that downstream profiles are flatter and more developed than those upstream of the expansion. That this is true can be seen in the velocity profile plots of Fig. 3. It is hypothesized that the profile upstream of the expansion is not quite fully developed because of slight tube-wall irregularities associated with the swirl generator's slots, pipe joints located at the swirl genera-

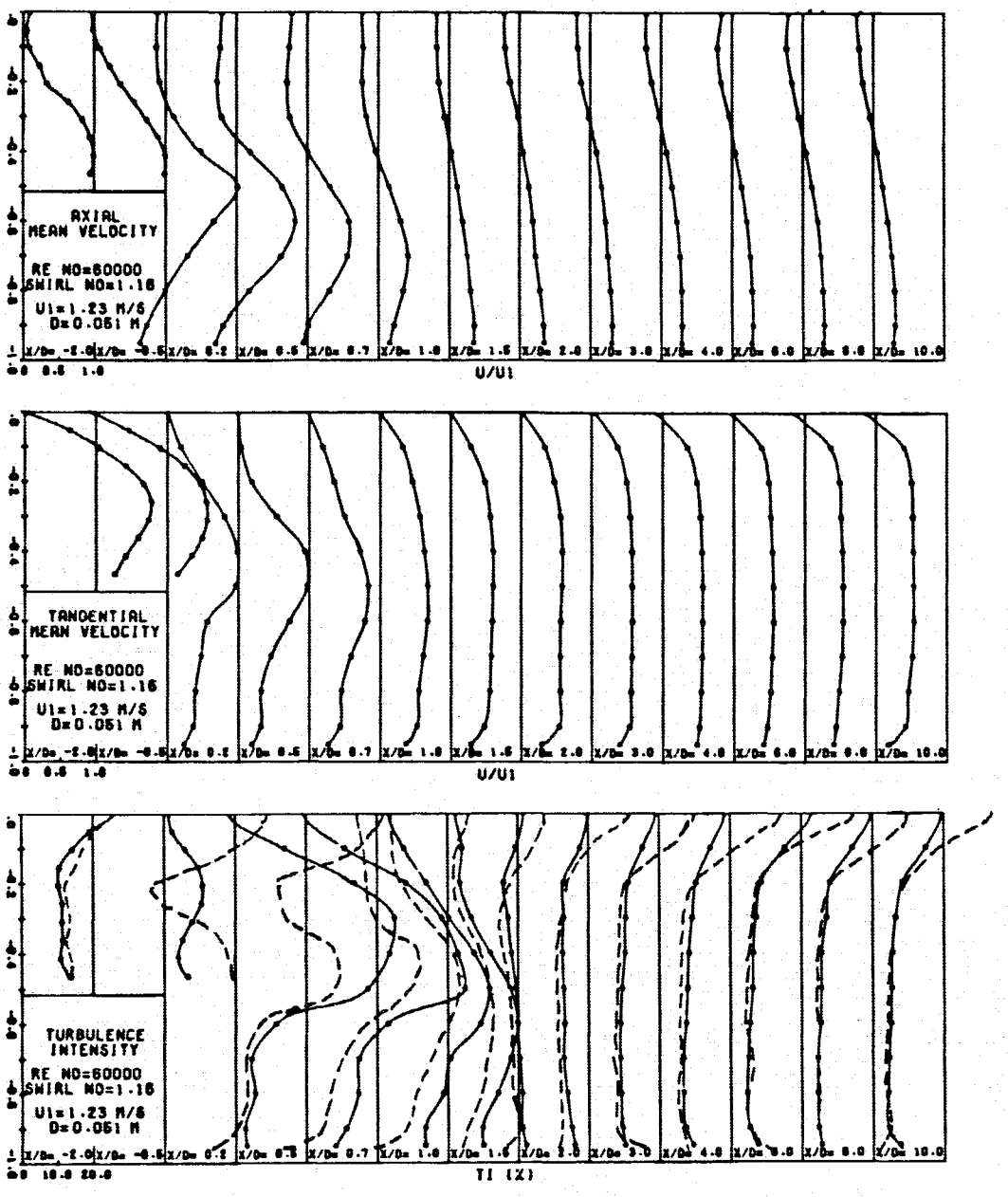

Fig. 6 Velocity field; $Re = 60{,}000$, $S = 1.16$: ——— axial TI; ---- tangential TI.

tor, and a flanged pipe connection approximately 4 diameters upstream of the $X/D = -2.0$ measuring station.

The normalized centerline velocity has no Reynolds number dependence for the unswirled flows. If we assume this also to be true for swirled flows, then Fig. 9 suggests that there is a swirl number between 0.74 and 0.98 that gives a maximum reverse velocity. Further, the maximum reverse velocity, which is seen to occur between $X/D = 0.5$ and $X/D = 1.3$, decreases in magnitude as swirl number is increased beyond $S = 0.98$. This suggests that there may be swirl numbers greater than 1.23 for which the centerline velocity may always be positive, as it is for the unswirled flows. Unfortunately, $S = 1.23$ was the upper limit on swirl strength available from the equipment used in this study, so that this hypothesis could not be investigated further.

For the present work, the position of $U = 0$ points at radial locations of $r/R_2 = 0.8$, 0.9, and 0.95 was determined by linear interpolation between adjacent grid points for which U had opposite signs. The $U = 0$ points from the three radial locations were then fitted with a spline and the resulting curve extrapolated to the wall to find the reattachment "point." Reattachment lengths obtained in this fashion for the present data are shown in Table 1. For the three unswirled cases, the reattachment lengths agree well with those reported for unswirled flows in the previously mentioned investigations (also shown in Table 1). We know of no existing data that can be used for comparison of reattachment lengths in swirled flows. When reattachment lengths are plotted against swirl number, the resulting curve is independent of Reynolds number and appears to be asymptotic to $x_r/h \approx 1.7$ as swirl number increases beyond 1.2. The reattachment lengths given here are actually average values determined from four to eight sets of velocity data obtained in the region of reattachment. The slight variations found in these velocities were sufficient to alter the computed lengths appreciably; this was especially true for the unswirled flows, where variations in reattachment length of ± 0.5 step height were not uncommon between individual data sets. The variation in reattachment length for the swirled cases was a more modest ± 0.1 step height for individual data trials. It is probably reasonable to consider these variations as repre-

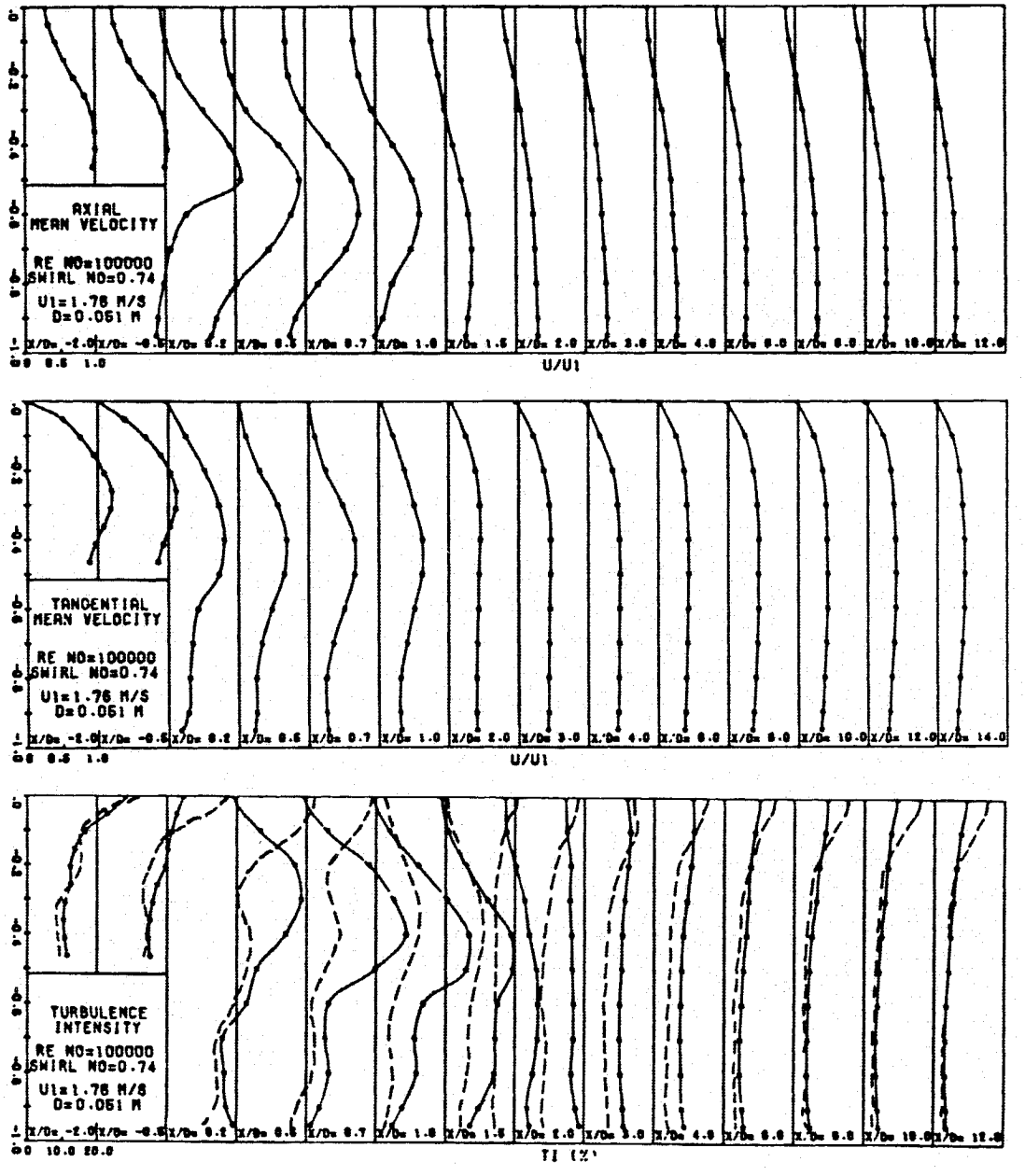

Fig. 7 Velocity field; $Re = 100{,}000$, $S = 0.74$: ——— axial TI; ----- tangential TI.

Table 2 Summary of flow regions

$Re = 30{,}000$	Remarks	$Re = 100{,}000$
$0 < S < 0.18$	Vortex precesses in direction opposite to the mean swirl	$0 < S < 0.12$
$S \approx 0.18$	Precession frequency goes to zero	$S \approx 0.12$
$0.18 < S < 0.37$	Vortex precesses in same direction as mean swirl	$0.12 < S < 0.40$
$S \approx 0.37$	PVC vanishes	$S \approx 0.40$
$0.37 < S < 0.50$	Bubble-type vortex breakdown	$0.40 < S < 0.57$
$S \approx 0.50$	Transition from recirculating bubble to strong on-axis tube of recirculating flow	$S \approx 0.57$
$S > 0.50$	Strong on-axis recirculation	$S > 0.57$

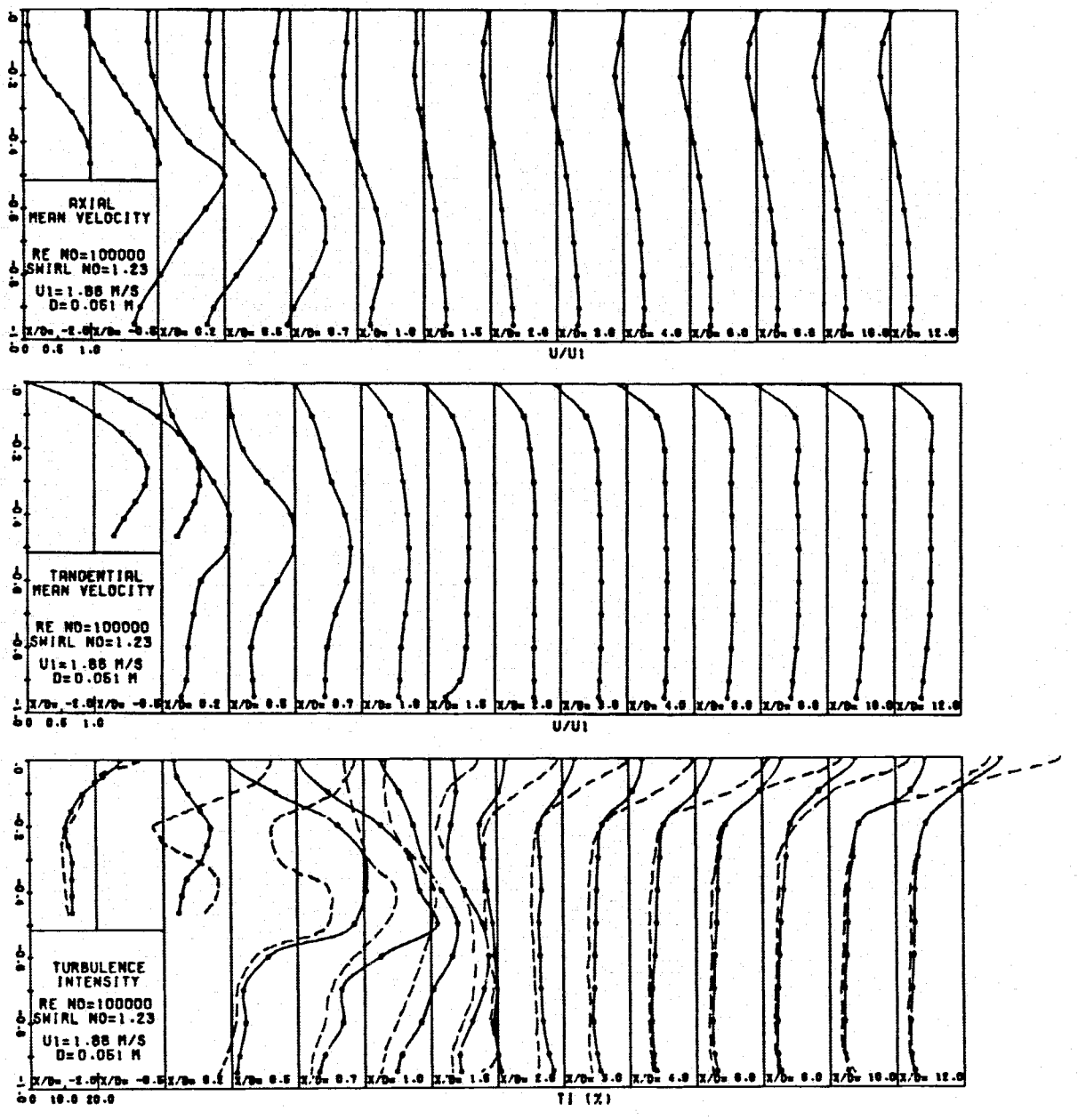

Fig. 8 Velocity field; Re = 100,000, S = 1.23: ——— axial TI; ---- tangential TI.

sentative of random fluctuations in the width of the reattachment zone rather than as an uncertainty in the measurement, but it is difficult to separate these two effects.

Mass balances obtained from integration of velocity profiles have become a commonly used standard for appraising the credibility of internal-flow velocity data. For a particular flow condition in the present work, the largest differences between the mass flux at any one profile and the average mass flux for all profiles (at that flow condition) were between 3 and 5%. The locations of poorest agreement were randomly scattered in the axial direction. Tabular velocity data and further details are available in the dissertation by Dellenback.[33]

PVC and Vortex Breakdown

Information that can be generalized about swirling-flow asymmetries and the PVC from previous studies is very sparse, largely because of the complexity of the flow's structure. Historically, the most easily and commonly measured feature of these asymmetries has been the relationship between the swirl number and precession frequency. This relationship also constitutes the principal result of the present study of the PVC. Although the computation of swirl number requires knowledge of the mean velocity profiles, which are not known a priori, the swirl number can also be related to the ratio of mass fluxes entering the swirl generator. For weakly swirled flows ($S < 0.15$), the swirl number was obtained from an algebraic relationship[6] between the axial and tangential mass fluxes that results from assuming plug flow with superimposed solid-body rotation. A second, experimentally determined relationship between the mass-flow ratio and the swirl number (from integrated velocity profiles) was deduced for higher swirl numbers. Precession frequencies were examined only at the two limiting Reynolds numbers of 30,000 and 100,000.

Precession-frequency data are combined with flow-visualization observations to summarize vortex breakdown and the PVC's swirl-dependent behavior in Table 2. Previous investigations have found that swirling flow asymmetries usually precess in the same direction as the mean swirl for confined flows and in the opposite direction for freejets. However, Escudier[25] reports that his sudden expansion data contradict this general

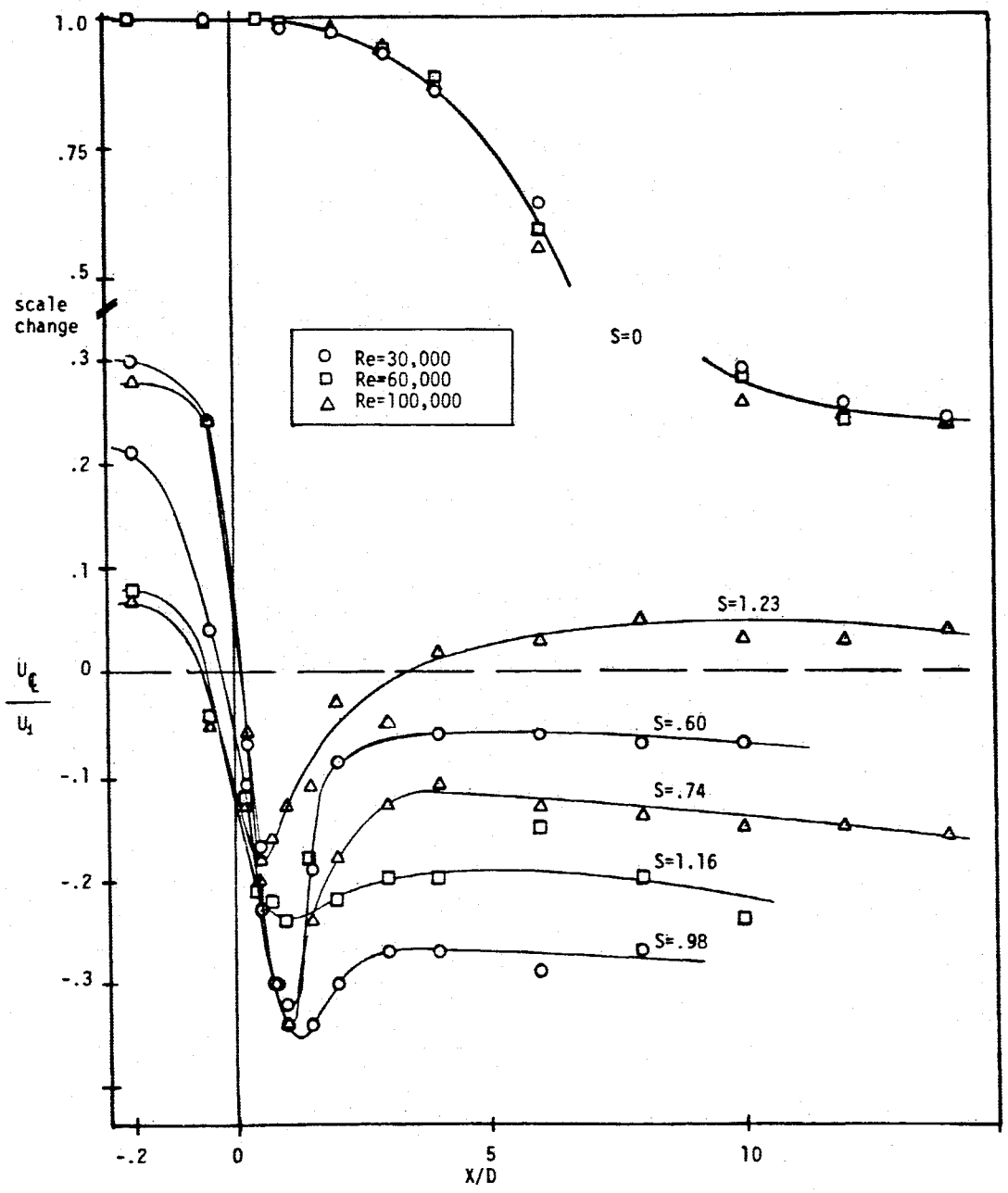

Fig. 9 Centerline velocities.

rule. In the present experiments, the PVC precessed with the mean swirl for larger swirl numbers, and against the mean swirl for low swirl numbers. Table 2 shows that although results for the two Reynolds numbers are similar, specific events occur at slightly different swirl numbers. Two regions were especially difficult to resolve. These were the precession frequencies for very low swirl ($S < 0.1$) and the swirl number at which the direction of precession changes. On the other hand, two points that had very sharp transitions as the swirl number was changed were the transition from PVC to vortex breakdown and the transition from a bubblelike vortex breakdown to a full-length tube of recirculating fluid on the tube centerline. Throughout the regime of swirl numbers for which the vortex-breakdown bubble exists, considerable unsteadiness of the bubble's location was noted in both the flow visualization and LDA data. This unsteadiness made it impossible to measure accurately either the velocities inside the bubble or the bubble's dimensions, but it was noted that the bubble extended to about $2\frac{1}{4}$ D downstream of the expansion. Downstream of the bubble, it was observed that although fluid on the tube axis was mostly stagnant in the mean, it was also quite unsteady, sometimes showing a tendency to drift randomly either upstream or downstream. When the PVC was present, flow oscillations could be detected at the upstream station of $X/D = -0.5$, but not further upstream at $X/D = -2.0$. Although several of the investigations cited previously observed the PVC at supercritical-swirl numbers, the PVC in the present study could be detected only at subcritical-swirl numbers. Finally, none of the results shown in Table 2 displayed any apparent hysteresis in swirl number.

Frequency information taken from the stripcharts (or spectrum analyzer, which agreed closely) was converted to Strouhal numbers[23] (fD^3/Q where f is the precession frequency and Q the volumetric flow rate) and used to generate Fig. 10. The scarcity of data points for $S < 0.1$ and near the zero-frequency crossovers is illustrative of the previously mentioned inability to resolve frequencies at these transitory swirl numbers. Away from these swirl numbers, smooth curves drawn through the available data points fit well and thus give confidence in extrapolating the swirl number for the zero frequency crossovers. Figure 10 also shows clearly the dependency of the precession frequency on Reynolds number.

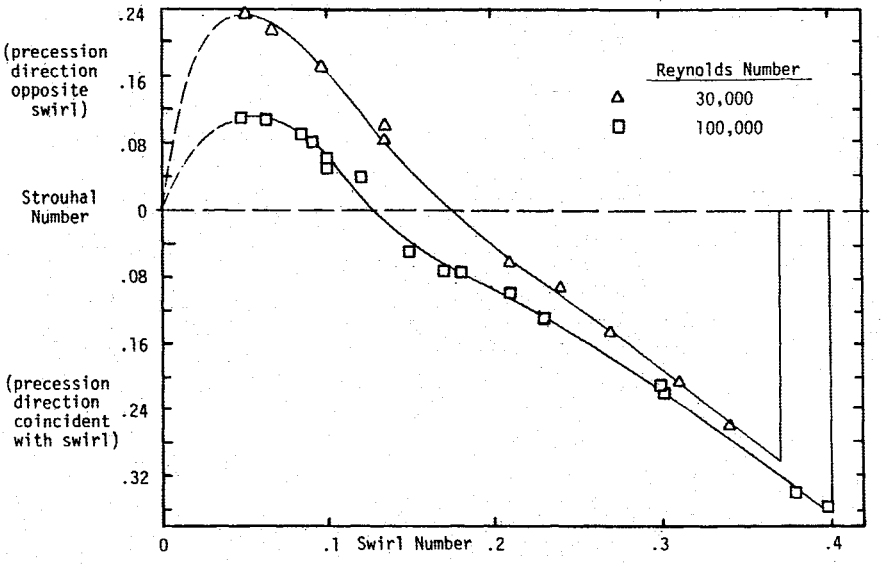

Fig. 10 Variation of Strouhal number with swirl number.

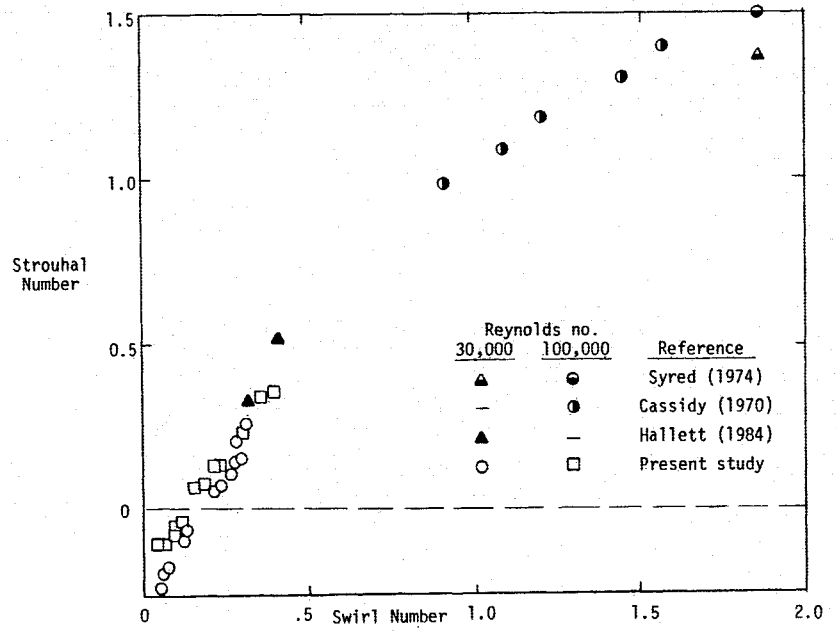

Fig. 11 Relationship between Strouhal number and swirl number (various experiments).

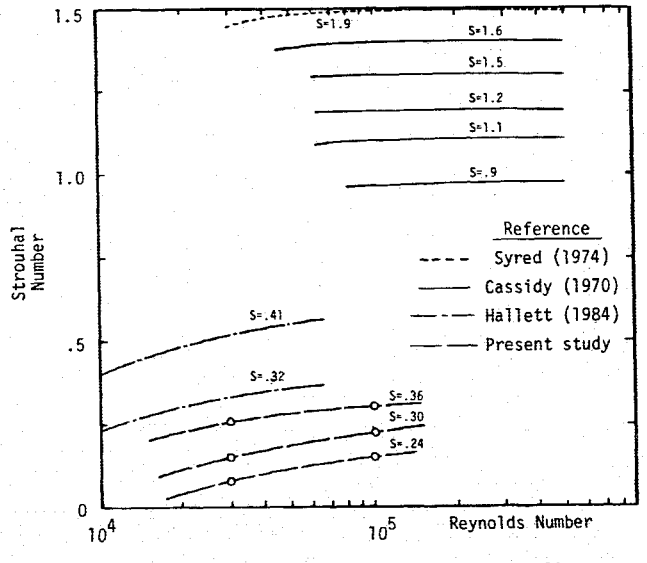

Fig. 12 Relationship between Strouhal number and Reynolds number (various experiments).

The frequencies of precession seem to follow a trend consistent with other investigations of asymmetries in swirling flows as shown by Figs. 11 and 12. Although the experiments of Syred and Beer[24] and Cassidy and Falvey[23] were in dissimilar geometries (freejet; straight tube and sudden contraction, respectively) and the PVC occurred in conjunction with vortex breakdown, there is a noticeable congruence of results in Fig. 12. In particular, the Strouhal number appears to be independent of Reynolds number for $Re > 10^5$, but a slowly decreasing function of Reynolds number at lower values of this parameter.

Closing Remarks

The principal contribution of the present study has been to quantify the magnitudes of mean and fluctuating velocities as a function of swirl and Reynolds numbers in an abrupt axisymmetric-expansion flow. In addition, a number of qualitative trends and features have been observed that may contribute in a general way to the understanding of complex shear flows. Documentation of the velocity field in the upstream tube should be helpful to computational flow modelers, and of general interest in light of how vastly the upstream flow changes just before reaching the expansion. For low swirl levels, an

unsteady, three-dimensional flow asymmetry has been observed. The asymmetry is such a complex flow structure that only a limited number of useful measurements can be obtained which help to specify its structure. At the higher swirl levels, the flow becomes symmetric, and extraordinarily high levels of turbulence are produced. The on-axis recirculation normally associated with highly swirled flows changes such that on-axis flow is in the downstream direction, with recirculation just off-axis.

Acknowledgment

This research was supported by the Office of Naval Research.

References

[1]Spalding. D. B., "Heat Transfer from Turbulent Separated Flows," *Journal of Fluid Mechanics,* Vol. 27, Pt. 1, 1967, pp. 97–109.

[2]Johnston, J. P., "Internal Flows," *Turbulence: Topics in Applied Physics*, 12th ed., Springer-Verlag, New York, 1978, pp. 144–152.

[3]Baughn, J. W., Hoffman, M. A., Takahashi, R. K., and Launder, B. E., "Local Heat Transfer Downstream of an Abrupt Expansion in a Circular Channel with Constant Wall Heat Flux," *Transactions of the ASME, Journal of Heat Transfer*, Vol. 106, Nov. 1984, pp. 789–796.

[4]Faler, J. H. and Leibovich, S., "Disrupted States of Vortex Flow and Vortex Breakdown," *Physics of Fluids*, Vol. 20, No. 9, Sept. 1977, pp. 1385–1400.

[5]Hallett, W. L. H. and Gunther, R., "Flow and Mixing in Swirling Flow in a Sudden Expansion," *Canadian Journal of Chemical Engineering*, Vol. 62, Feb. 1984, pp. 149–155.

[6]Gupta, A. K., Lilley, D. G., and Syred, N., *Swirl Flows*, Abacus Press, Tunbridge Wells, Kent, England, 1984.

[7]Sultanian, B. K., Neitzel, G. P., and Metzger, D. E., "Turbulent Flow Predictions in a Sudden Axisymmetric Expansion," *Proceedings of the International Symposium on Refined Flow Modeling and Turbulence Measurements*, 1985.

[8]Chaturvedi, M. C., "Flow Characteristics of Axisymmetric Expansions," *Journal of the Hydraulics Division—Proceedings of the American Society of Civil Engineers*, Vol. HY 3, 1963, pp. 61–92.

[9]Freeman, A. R., "Laser Anemometer Measurements in the Recirculating Region Downstream of a Sudden Pipe Expansion," *Accuracy of Flow Measurements by Laser Doppler Methods—Proceedings of the LDA Symposium*, 1975, pp. 704–709.

[10]Moon, L. F. and Rudinger, G., "Velocity Distribution in an Abruptly Expanding Circular Duct," *Transactions of the ASME, Journal of Fluids Engineering*, Vol. 99, March 1977, pp. 226–230.

[11]Yang, B. T. and Yu, M. H., "The Flowfield in a Suddenly Enlarged Combustion Chamber," *AIAA Journal*, Vol. 21, Jan. 1983, pp. 92–97.

[12]Gould, R. D., Stevenson, W. H., and Thompson, H. D., "Laser Velocimeter Measurements in a Dump Combustor," American Society of Mechanical Engineers Paper 83-HT-47, 1983.

[13]Stevenson, W. H., Thompson, H. D., and Gould, R. D., "Laser Velocimeter Measurements and Analysis in Turbulent Flows with Combustion, Part II," Air Force Wright Aeronautical Laboratories TR-82-2076, 1983.

[14]Sultanian, B. K., "Numerical Modeling of Turbulent Swirling Flow Downstream of an Abrupt Pipe Expansion," Ph.D. Dissertation, Arizona State Univ., Tempe, AZ, 1984.

[15]Gosman, A. D., Khalil, E. E., and Whitelaw, J. H., "The Calculation of Two-dimensional Recirculating Flows," *Turbulent Shear Flows*, Vol. 1, Springer-Verlag, New York, 1977, pp. 237–254.

[16]Minh, H. H. and Chassaing, P., "Perturbations of Turbulent Pipe Flow," *Turbulent Shear Flows*, Vol. 1, Springer-Verlag, New York, 1977, pp. 178–197.

[17]Jackson, T. W. and Lilley, D. G., "Single-wire Swirl Flow Turbulence Measurements," AIAA Paper 83-1202, June 1983.

[18]Janjua, S. I., McLaughlin, D. K., Jackson, T. W., and Lilley, D. G., "Turbulence Measurements in Confined Jets Using a Rotating Single-wire Probe Technique," *AIAA Journal*, Vol. 21, Dec. 1983, pp. 1609–1610.

[19]Rhode, D. L., Lilley, D. G., and McLaughlin, D. K., "Mean Flowfields in Axisymmetric Combustor Geometries with Swirl," *AIAA Journal*, Vol. 21, April 1983, pp. 593–600.

[20]Abujelala, M. T., Jackson, T. W., and Lilley, D. G., "Swirl Flow Turbulence Modeling," AIAA Paper 84-1376, June 1984.

[21]Hall, M. G., "Vortex Breakdown," *Annual Review of Fluid Mechanics*, Vol. 4, Annual Reviews, Palo Alto, CA, 1972, pp. 195–218.

[22]Leibovich, S., "Vortex Stability and Breakdown: Survey and Extension," *AIAA Journal*, Vol. 22, Sept. 1984, pp. 1192–1206.

[23]Cassidy, J. J. and Falvey, H. T., "Observations of Unsteady Flow Arising After Vortex Breakdown," *Journal of Fluid Mechanics*, Vol. 41, Pt. 4, 1970, pp. 727–736.

[24]Syred, B. and Beer, J. M., "Combustion in Swirling Flows: A Review," *Combustion and Flame*, Vol. 23, 1974, pp. 143–201.

[25]Escudier, M. P., "Observations of Confined Vortices," *Flow Visualization*, Vol. II, 1980, pp. 379–383.

[26]Sarpkaya, T., "On Stationary and Travelling Vortex Breakdowns," *Journal of Fluid Mechanics,* Vol. 45, Pt. 3, 1971, pp. 545–559.

[27]Melling, A. and Whitelaw, J. H., "Optical and Flow Aspects of Particles," *Accuracy of Flow Measurements by Laser Doppler Methods—Proceedings of the LDA Symposium*, 1975, pp. 382–392.

[28]Boadway, J. D. and Karahan, E., "Correction of Laser Doppler Anemometer Readings for Refraction at Cylindrical Interfaces," *DISA Information*, No. 26, DISA Electronics, Franklin Lakes, NJ, 1981, pp. 4–6.

[29]Durao, D. F. G., Laker, J., and Whitelaw, J. H., "Bias Effects in Laser Doppler Anemometry," *Journal of Physics E: Scientific Instruments*, Vol. 13, 1980, pp. 442–445.

[30]Bates, C. J. and Hughes, T. D. R., "The Effect of Both Sample Size and Sampling Rate on the Statistical Fluid Flow Parameters in a High Reynolds Number, Low Turbulence Intensity Flow," *Symposium on Turbulence*, 1977, pp. 125–131.

[31]Karpuk, M. E. and Tiederman, W. G., "Effect of Finite-size Probe Volume Upon LDA Measurements," *AIAA Journal*, Vol. 14, Aug. 1976, pp. 1099–1105.

[32]Kline, S. J. and McClintock, F. A., "Describing Uncertainties in Single-sample Experiments," *Mechanical Engineering*, Vol. 75, No. 1, 1953, pp. 3–8.

[33]Dellenback, P. A., "Heat Transfer and Velocity Measurements in Turbulent Swirling Flow Downstream of an Abrupt Axisymmetric Expansion," Ph.D. Dissertation, Arizona State Univ., Tempe, AZ, 1986.